X-Ray-Generated Ultrasonic Signals: Characteristics and Imaging Applications

WOLFGANG SACHSE, MEMBER, IEEE, KWANG YUL KIM, AND WILBUR F. PIERCE

Abstract—**Experiments dealing with the characterization of X-ray-generated ultrasonic signals in materials and their application to the imaging of material inhomogeneities are described. A linear relationship is established between the X-ray photon power and the generated ultrasonic signals. The directivity of the X-ray/acoustic source was found to resemble that of other thermoelastic sources. A new double-modulation measurement technique is described in which the magnitude and phase of the modulated acoustic signals are measured. Use of the technique is explored with various materials, incident beam sizes, and inclusions. The results of preliminary imaging experiments are described which were carried out with direct and double-modulated X-ray/acoustic signals. The measured images exhibit features dominated by the effects of the transducer and elastic wave resonances in the specimens. It is shown from these results that using the images generated at two modulation frequencies, identification of the spatial inhomogeneities in a specimen is possible.**

I. Overview

THE USE of short-duration thermal sources to generate elastic waves in solids is rapidly becoming widely accepted as the basis of new ultrasonic measurement and material-microstructure imaging techniques. A general overview of such ultrasonic sources is given in [1] with extensive additional details, specific to laser-generated ultrasonic signals, contained in [2] and [3]. Investigated in detail has been the modeling of the laser/ultrasonic source as a function of various operational parameters including the incident energy, the beam size, and the effect of a constraining layer on the target region of a specimen in addition to the thermal and mechanical properties of the specimen material. Other publications have reported preliminary results of the application of such sources as the basis of a noncontact, point source of ultrasonic waves in solids for materials testing applications [3], [4]. Since the thermal excitation is a pulse, typically of submicrosecond duration, the sound source is localized within a few microns of the surface in most materials, thus facilitating time-of-flight and ultrasonic velocity measurements [5].

The use of a pulsed or modulated continuous-wave thermal source in a scanning mode over a specimen forms the basis of imaging techniques which may be based on thermal or thermoelastically generated acoustic waves, depending on the signal detection method employed [6], [7]. For cases in which the pulse duration and repetition period are in the msec range, the region of thermomechanical interaction may extend typically from 0.1 to several millimeters into the interior, permitting near-surface microstructural features to be imaged with thermal waves. Material inhomogeneities on the surface or through the interior of a material can also be imaged with the thermoelastically generated acoustic waves. An important difference, however, between the thermal and the acoustic waves is that the wavelength of the latter is typically a thousand times greater than the former [7]. The use of other pulsed thermal sources to generate ultrasonic waves in solids has also been actively explored. These include electrical arcs [8], pulsed electron [9], and ion [10] beams, among others.

In view of this, the recent discovery of X-ray-generated ultrasonic signals [11], [12] is not surprising. But in contrast to the earlier sources, X-rays, which are exceptionally short wavelength photons, can penetrate into the interior of a material to a depth related to the mass absorption coefficient, which depends on the X-ray wavelength and the specimen material's atomic number. For an X-ray beam of typically 10 keV, the mean decay depth (that is, the distance in which X-ray intensity decays by a factor of $1/e$) is about 0.14 mm in a light absorber such as aluminum. Thus it is possible that in certain testing configurations, the associated ultrasonic source may be distributed over a region in the interior of a solid. In contrast, when a laser is used as a source, the classical skin depth is approximately 3.76 nm.

It is natural then to inquire about the mechanisms which play a role in the generation of ultrasonic signals in a solid by an intense, pulsed X-ray source and how the associated contrast mechanisms can be used to image and characterize the microstructures of materials. This paper describes research which has investigated such phenomena. In Section II we describe details of the experimental system for generating, detecting, and processing X-ray/acoustic signals from the specimens used. Section III contains the results of experiments investigating the characteristics of the X-ray/acoustic source and the generated ultrasonic signals. In Section IV we describe the first results of imaging material inhomogeneities with X-ray-generated ultrasonic signals while some concluding remarks are in Section V.

Manuscript received March 12, 1986; revised April 10, 1986. This work was supported by the Physics Division of the Office of Naval Research, the Materials Science Center of Cornell University, and the National Science Foundation.

The author is with the Department of Theoretical and Applied Mechanics, Cornell University, Ithaca, NY 14853, USA.

IEEE Log Number 8609267.

0885-3010/86/0900-0546$01.00 © 1986 IEEE

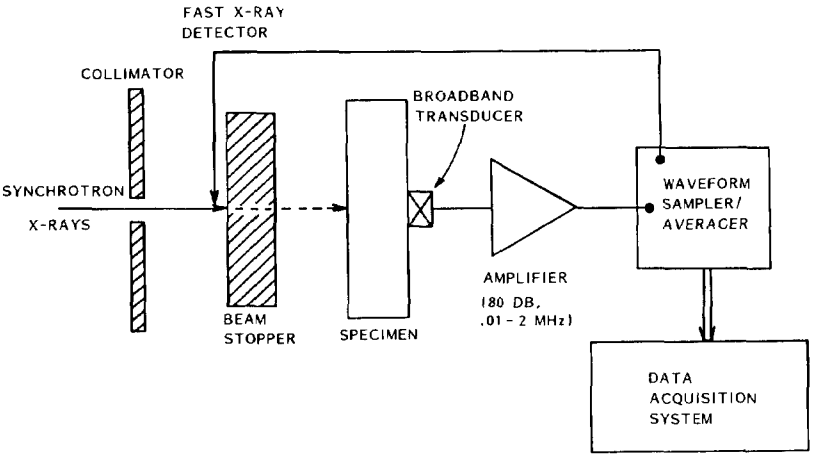

Fig. 1. Schematic of experimental setup for detecting X-ray/generated ultrasonic signals.

II. Measurement System

Synchrotron radiation is emitted when particles such as positrons and electrons traveling at nearly the speed of light in a high vacuum are accelerated in a curved path in a magnetic field. The principal characteristics of this radiation include its high intensity, broad spectral range, high polarization, pulsed time structure, and natural collimation. At Cornell, such a high-energy synchrotron source (Cornell high energy synchrotron source (CHESS)) operates in a parasitic mode to an electron-storage-ring facility. The generated X-rays possess a uniform, broadband spectrum up to a critical energy of 10 keV, decreasing exponentially at higher energies. The X-rays appear as intense pulses of 0.160 ns duration at a repetition rate determined by the period of motion of the particle "bunches" circulating in the storage ring of the synchrotron. The beam energy in each X-ray pulse is typically 8.0 μJ/per horizontal milliradian which after collimation results in a pulsed X-ray beam with about 1.12 μJ/pulse incident on a specimen.

The inherent pulsed nature of synchrotron-generated X-rays is ideal for making time-resolved studies. In our early experiments, the synchrotron was generating X-ray pulses at a repetition frequency of 390.6 kHz. This provided a time window for listening 2.56 μs in duration, which was sufficient for clearly identifying of particular ultrasonic wave arrivals in the detected waveforms. Unfortunately, during the course of the experiments, the operation of the synchrotron was modified to give two additional pulses equi-spaced between the original ones. Hence the excitation repetition period was reduced to approximately 850 ns, which precludes the identification of individual wave arrivals and places restrictions on the data processing schemes that can be successfully implemented.

As with other thermoacoustic measurements, the essential components needed to detect X-ray-generated ultrasonic signals in a material involve a transducer, amplifier and signal recording and acquisition system as shown in Fig. 1.

In the experiments to be described, the ultrasonic signals were detected with broadband piezoelectric transducers possessing center frequencies between 1 and 7 MHz and having fractional bandwidths ranging from 80 to 120 percent. The specimen holding fixture had provisions for mounting the transducer at the epicentral position as well as on the edge of circular specimens. Various transducers with active elements 1.3–63 mm in diameter were used. The output of the transducers was amplified 60 to 80 dB by preamplifiers whose bandwidths ranged from approximately 10 kHz to 2 MHz. The low-frequency response of the transducer/amplifier combination was limited principally by the response of the transducers, while the high-frequency characteristics were governed by the preamplifiers. The frequency response of the system was determined by applying a step force directly on the transducer element and recording the output signal. The step force was obtained by breaking a glass capillary of 0.05-mm ID and 0.08-mm OD. The resultant signal risetime was less than 80 ns. Many transducer–amplifier combinations covering different frequency ranges were tried, but the choice of sensor and amplifier used in the experiments was determined by resolution and signal-to-noise factors.

The environment of the synchrotron is electrically and mechanically very noisy. To facilitate recording the waveforms with a maximum reduction of incoherent noise, the signals were either sequentially or randomly sampled via a sampling or digital processing oscilloscope, respectively. A fast photodiode whose risetime was less than 1 ns was used as an X-ray detector to generate a fast risetime electrical signal in synchronization with the appearance of the X-ray pulse at the exit of the beam pipe. Waveform acquisition was arranged to occur in synchronization with this pulse. This procedure effectively minimized the effects of all non-X-ray pulse-related mechanical and electrical noise.

The characteristics of the X-ray acoustic source were investigated by using specimens fabricated from readily available metals possessing a broad range of thermal and

X-ray absorption properties. Experiments were made on disk-like specimens 5.72 cm in diameter and 1.52 cm thick. The materials investigated included aluminum, brass, copper, mild and stainless steel, and titanium.

Among the other specimens tested, the results of two will be discussed here. They possessed particular geometries and were fabricated from aluminum. For investigating the directivity of the X-ray/acoustic source, an aluminum block 12.07 cm long, shaped as a semi cylinder of radius 4.76 cm with small, flat regions at 10° intervals on the outside surface was fabricated. Imaging measurements were made on a series of disk-like specimens fabricated 5.72 cm in diameter and 2.5 cm thick with side-drilled holes 1.59 mm in diameter through their interiors. These holes were drilled either parallel at various distances from the end faces or inclined from 1.6–15.5 mm to the end face. One specimen was made with two crossed holes 1.6 mm in diameter and 4.6 mm from the end face. Another specimen contained a plug of tool steel 19 mm long, which was force-fit into the central portion of the side-drilled hole 2.38 mm in diameter located 4.6 mm under the surface.

Results

A. X-Ray/Acoustic Signals

A composite plot of the signals detected in each of the metal samples during one repetition cycle of the synchrotron source comprises Fig. 2. Here the excitation repetition period was 2.56 μs. In these measurements the receiving transducer was mounted at the epicentral position and the signals were amplified equally and displayed to the same scale factor in the figure. The left edge of each time record corresponds to the interaction of the X-rays and the front surface of the specimen. The strong signal identified by P in each trace corresponds to the arrival of the longitudinal wave amplitude propagating once across the specimen thickness. The much smaller amplitude identified as S corresponds to the shear wave arrival from a previous excitation pulse. The wavespeeds in brass are so low that the pulses identified in the time record correspond to those which result from the excitation pulses of previous synchrotron cycles. The identification of particular wave arrivals at the appropriate arrival time in the ultrasonic time records is taken as clear evidence of X-ray generated ultrasonic signals.

The use of a constraining layer to enhance the generation efficiency of thermoelastic waves in a solid from an incident laser pulse is well known [13]. Experiments with "constraining" layers such as fluids, surprisingly produced no measurable signal enhancement. When thin metal foils (lead and aluminum, 0.15 mm thick with adhesive backing) covered the X-ray–specimen interaction region, the signal amplitudes did not increase significantly, but their characteristics were completely altered [12].

If the source of elastic waves resulting from the interaction of an intense beam of pulsed X-rays extends over

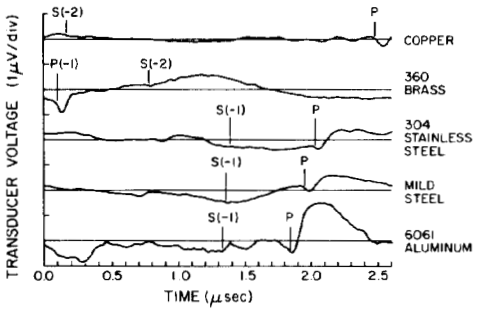

Fig. 2. X-ray/generated ultrasonic signals in various metals.

a finite dimension into the interior of a material, the source can be modeled on an assemblage of point sources [12]. If this is the case, determination of the X-ray–acoustic source strength in a specimen could form the basis of a new thermoelastic-wave imaging technique, which would be sensitive to subsurface microstructural features of a specimen. Algorithms for obtaining solutions to both the forward and inverse problems associated with an extended source have been developed [14]. In the solution to the inverse problem, the signal detected at a receiver point in the near field of a source can be processed to recover both the time-function of the source as well as its spatial extent. Based on the previous work with laser-acoustic sources, it can be expected that the source-time function of the X-ray–acoustic source approximates that of the Heaviside step function [2]. In that case, recovery of the spatial-dependence of the source strength can be obtained in a straightforward manner by simple deconvolution techniques, such as the successive substitution method [15]. Unfortunately, the existing signal-processing algorithms require the signal from just one event as input. With the high pulse repetition rate under which the synchrotron is currently operating, it is difficult to isolate in the received waveform those features corresponding to only one excitation. Also, the signals recorded in the earlier experiments are the voltage signals obtained from transducers whose transfer functions are unknown. This precludes recovery of the ultrasonic displacement signals, which are required as input to the available processing schemes. Thus evaluation of the extended source model of the X-ray/acoustic source is not now possible with either the existing or currently available ultrasonic waveform data available to us.

B. Verification of the X-Ray/Acoustic Source

In all of the initial experiments related to the discovery of the X-ray/acoustic effect, which were summarized in Fig. 2, the piezoelectric detection transducer was mounted at the epicentral receiver position relative to the X-ray target point on the specimen. A critical question to be addressed in the new experiments was related to the possibility that a portion of the transducer output signal was the result of a direct interaction between the X-ray beam and the detecting transducer. To check this, each of the circular disk-like specimens previously tested was re-

tested with a second point piezoelectric transducer 1.3 mm in diameter, which was mounted on the edge of the specimen and far removed from the direct path of the X-ray beam. A sample result obtained for aluminum is shown in Fig. 3. The results for all the other materials are similar.

As shown in the figure and observed in all others, the acquired waveforms at epicenter and off-epicenter are dominated by the new, higher X-ray pulse repetition rate of 1.2 MHz compared to the signals shown in Fig. 2. The result is a quasi-harmonic, periodic output signal in which it is very difficult to identify the arrivals of particular wave modes. It was noted that the amplitudes of the signals detected on the aluminum specimen appear to be lower than those obtained on a steel specimen. However these differences can be accounted for if the instantaneous synchrotron beam current, and hence the incident photon power, is taken into account and if the transducer/specimen coupling could be made identical in all cases.

Another noticeable difference between the signals obtained in the different materials is the apparent phase shift between the epicentral and off-epicentral signals. This effect can be explained from consideration of the phase velocity difference between the various specimen materials. For example, in aluminum, the phase shift between the epicentral and off-epicentral signals is 224° while for steel the corresponding value is 12°.

C. Beam Current Dependence

One factor complicating all the X-ray/acoustic measurements is that the beam current of the electron bunches circulating in the storage ring, which is directly related to the X-ray photon power incident on a specimen, decreases with time and must be replenished by a "fill." Immediately after a fill, the beam current of the Cornell synchrotron is typically 40 mA decreasing to approximately 18 mA near the end of a one-and-a-half-hour run. The incident photon power correspondingly decreases from approximately 1.96 to 0.9 W after collimation, depending on synchrotron operating conditions.

To determine the relationship between the beam current and the detected acoustic signals, measurements were made on each of the specimens tested earlier, while changes in the acoustic waveforms were monitored as the beam current decreased during a run. At each measurement, one hundred acoustic waveforms were averaged. From this average the rms, peak-to-peak voltage, and energy values of the signals generated at each electron-beam-current value were extracted. The results obtained on the stainless steel specimen are shown in Fig. 4. It is observed that the decrease in signal rms amplitude with beam current is nearly linear with a nonzero intercept. The reason for the latter has not yet been determined. The initial high-beam current portions of the curves exhibit a complicated behavior that appears to be related to tuning operations performed on the beam by the synchrotron operators.

It should also be mentioned that in some cases an anomalous behavior was observed during a run. This was often

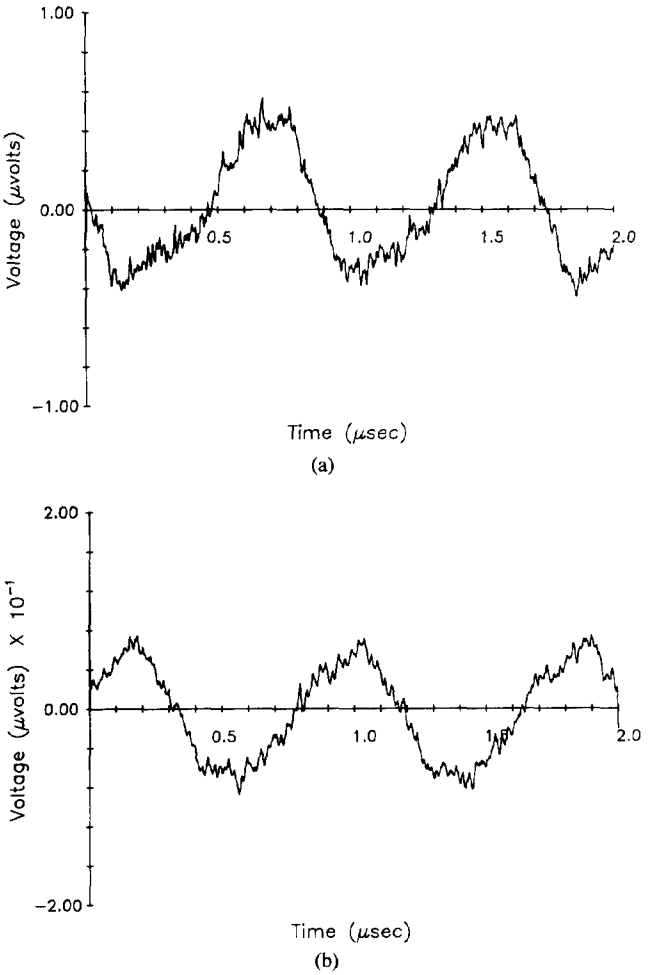

Fig. 3. X-ray/acoustic signals in aluminum. (a) Epicentral transducer signal. (b) Side-mounted transducer signal.

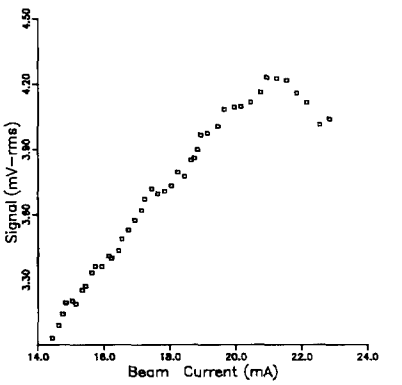

Fig. 4. rms signal beam-current dependence in stainless steel.

related to cases in which the signals were small in amplitude, possibly resulting from a poor transducer–specimen bond, incomplete tuning of the X-ray beam, or improper adjustment of the exit point of the X-ray beam from the synchrotron. The results obtained for another stainless steel specimen are shown in Figs. 5(a)–(c). The abscissa is given in terms of a voltage with 1.0 volts corresponding to 40 mA of beam current. The last figure shows a jump in the signal output, which appears to be related to the

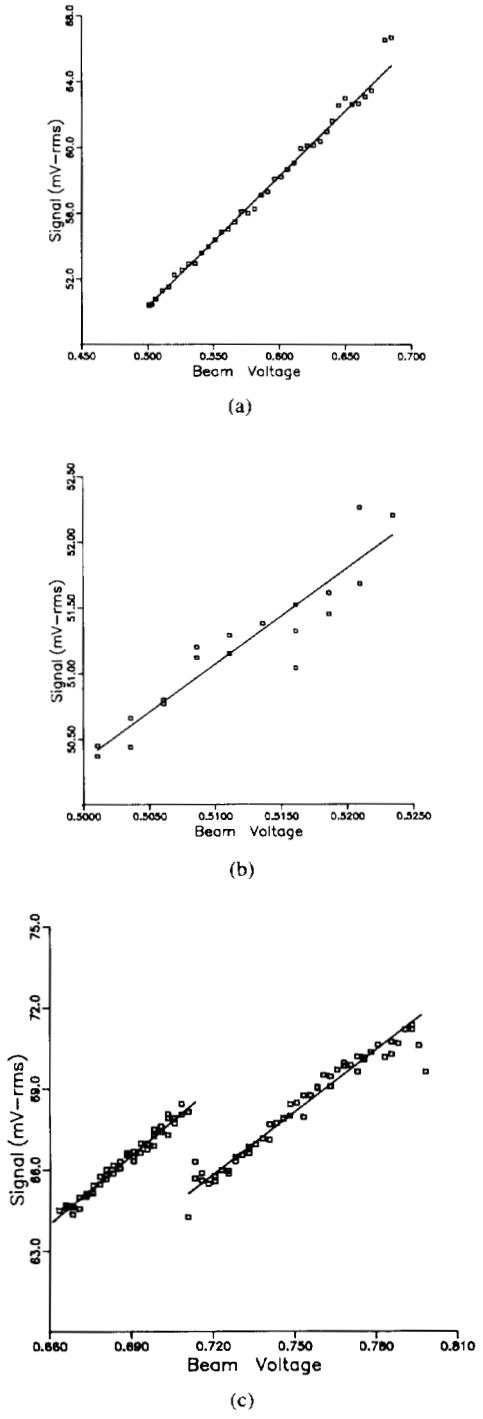

Fig. 5. X-ray/acoustic signal, beam-current dependence in stainless steel. (a) no. 1. (b) no. 2. (c) no. 3.

operational characteristics of the synchrotron. These observations suggest a possible application of the X-ray–acoustic phenomenon as the basis of an X-ray beam monitor sensor, sensitive to the X-ray photon power incident on a material.

The result of one test in brass consisting of more than 160 data points, spanning a very broad range of beam currents, exhibited a nonlinear behavior. This may not be typical and another test of this material is needed.

A linear least-squares fit was made with the results obtained for each specimen to recover a value of the signal decay rate as well as the intercept value. A compilation of the signal rms decay rates and intercepts extracted from what are believed to be the most reliably measured decay curves is listed in Table I. The number in parenthesis following some of the data values indicates the number of tests included in the figure. The signal-decay curves generated when the peak-to-peak voltage or energy of the waveform is plotted yield similar results.

TABLE I
SIGNAL RMS DECAY RATES AND INTERCEPTS

Parameter	Brass	Stainless Steel	Titanium	Copper	Mild Steel
Signal rms Decay rate (mV/beam volts)	83.9	75.9 (2)	91.4 (2)	51.8	90.6 (2)
Intercept (mV rms)	1.2	12.4 (2)	−1.1(2)	22.4	12.0 (2)

D. Beam-Size Dependence

The dependence of the X-ray/acoustic signals on the beam size was also determined. To investigate this, two brass plates 0.5 inches thick were used to form a horizontal beam aperture. The plates were mounted on translation stages which could be moved with actuators from a closed position to open more than 30 mm with a reproducibility better than one micrometer. The vertical extent of the beam was fixed at approximately 2 mm by slits which form an integral part of the beam pipe. Specimens of aluminum and brass were measured with data collected every 2 mm of aperture during both opening and closing of the aperture.

The rms and peak-to-peak voltage values of the X-ray/acoustic signals generated in a brass specimen are shown in Figs. 6(a)–(b). The waveforms were detected with a transducer 18.8 mm in diameter mounted on the back side of the specimen. Immediately apparent is the linear increase in signal amplitude with increasing aperture. As expected, there is no further increase in the signal amplitude when the aperture exceeds the size of the transducer. At very small apertures there appear to be some nonlinearities present which are still unexplained. A comparison of the aperture effect on the peak-to-peak values of the signals detected with the same transducer in brass and aluminum specimens is shown in Fig. 7. Superimposed is the linear least-square analysis of this data, which demonstrates that over most of the aperture range relation between the generated signal and aperture is linear. The slope obtained for brass is 19.2 mV per millimeter of aperture; while the slope for aluminum is 14.5 mV per millimeter of aperture. But these values can be expected to be affected by specimen/transducer coupling effects and by intensity variations of the excitation beam resulting from tuning operations. The intercept in every case is nonzero.

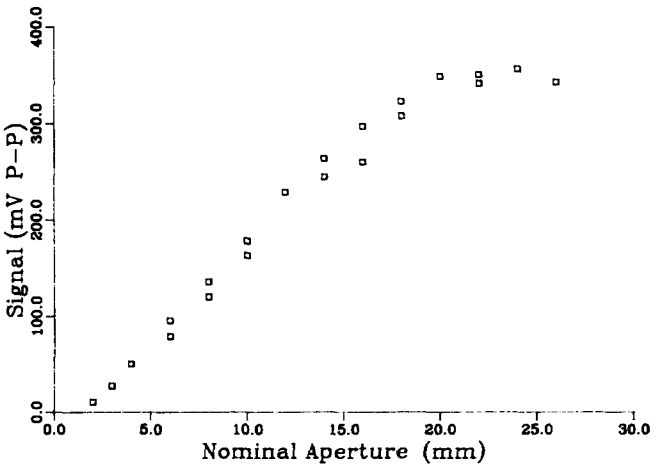

(a)

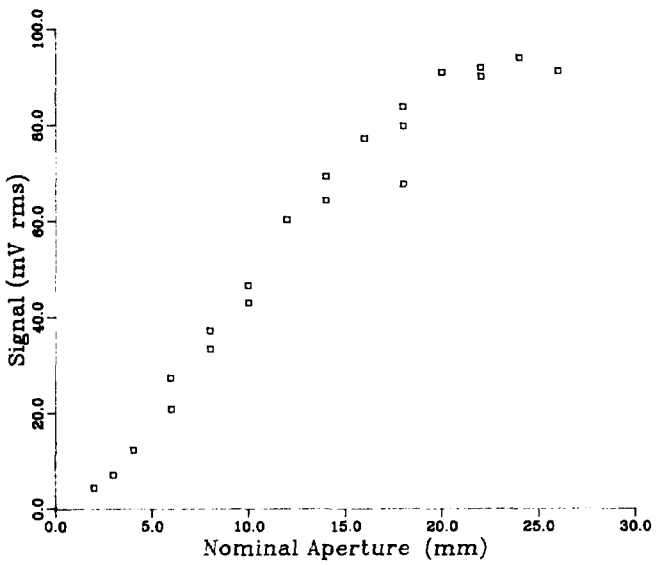

(b)

Fig. 6. X-ray/acoustic-signal/beam-aperture dependence in brass. (a) rms signal. (b) Peak-to-peak voltage signal.

From our earlier work on extended acoustic sources in materials it was anticipated that as the size of the X-ray/acoustic source increases, the generated signals should exhibit an increase in the risetime of the amplitudes corresponding to particular ray arrivals in the waveforms [14]. Our inability to identify specific wave arrivals in the detected signals precluded a direct check of this as the X-ray beam aperture was increased. Instead, use of an alternate procedure was explored which is based on measurement of the Fourier spectra of the acoustic waveforms. It is known that the phase spectra are directly related to the phase and group delay of the signals propagating through a specimen of length L [16]. For waves in nondispersive media, it is presumed that if the measured phase difference is frequency-dependent, information regarding the extent of the acoustic source is contained in the phase spectrum. That is, it should be possible to extract from the phase function an effective source-receiver distance. That is, as the size of the X-ray/acoustic source increases in a specimen, the distance between source and receiver will decrease.

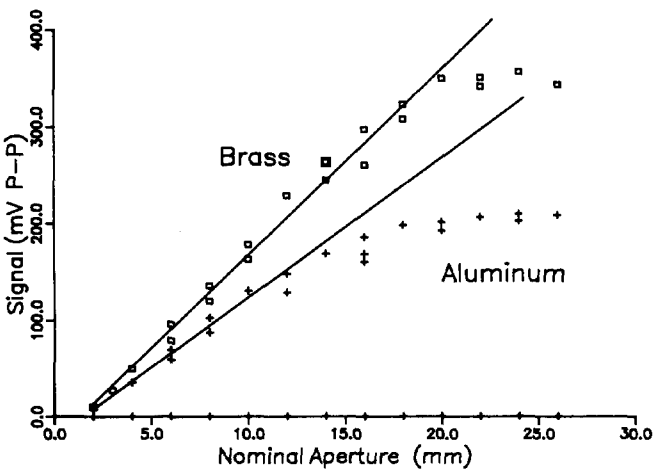

Fig. 7. Peak-to-peak signal/beam aperture effect in brass and aluminum.

To test this, the waveforms recorded at different apertures were windowed to obtain one cycle and Fourier-transformed. Shown in Figs. 8(a)–(d) are the signals measured at two X-ray beam apertures, 4 mm and 24 mm, in aluminum. Also shown are the Fourier magnitudes, their unwrapped phase spectra and the phase difference between them. The difference in the phase functions of the signals generated through the two apertures which is shown in Fig. 8(d) indicates that the position of the thermoelastic source resulting from the larger aperture differs from that of the smaller source. If this model is correct, the average measured phase difference is 0.45 rad, which corresponds to a difference in the position of the thermoelastic source in these two cases of approximately 0.4 mm.

E. Signal Directivity

The directivity of a source of elastic waves is a parameter that gives essential information about the nature of the source and, hopefully, in the X-ray/acoustic case, the nature of the X-ray/material interaction process. For quantitative ultrasonic measurements it is also essential that the source directivity be known so that waveform amplitude measurements, which are made at off-axis positions, can be properly compensated.

To determine the directivity pattern of the X-ray/acoustic source, the semicircular specimen of aluminum was used. Seventeen flat areas were machined on the circular surface such that small point piezoelectric transducers of 1.3 mm active area could be properly mounted to detect the radiated signals at points equi-distant from the source at 10° intervals in the sound field. To calibrate the system, provision was made for attaching a piezoelectric point transducer operating as a source, at the X-ray source point and detecting the amplitudes of specific features or the entire waveform, if desired, at each of the receiver points. In Fig. 9(a)–(d) are shown four X-ray-generated signals detected at every 30° on the specimen. It is seen that, as expected, the signals are dominated by the exci-

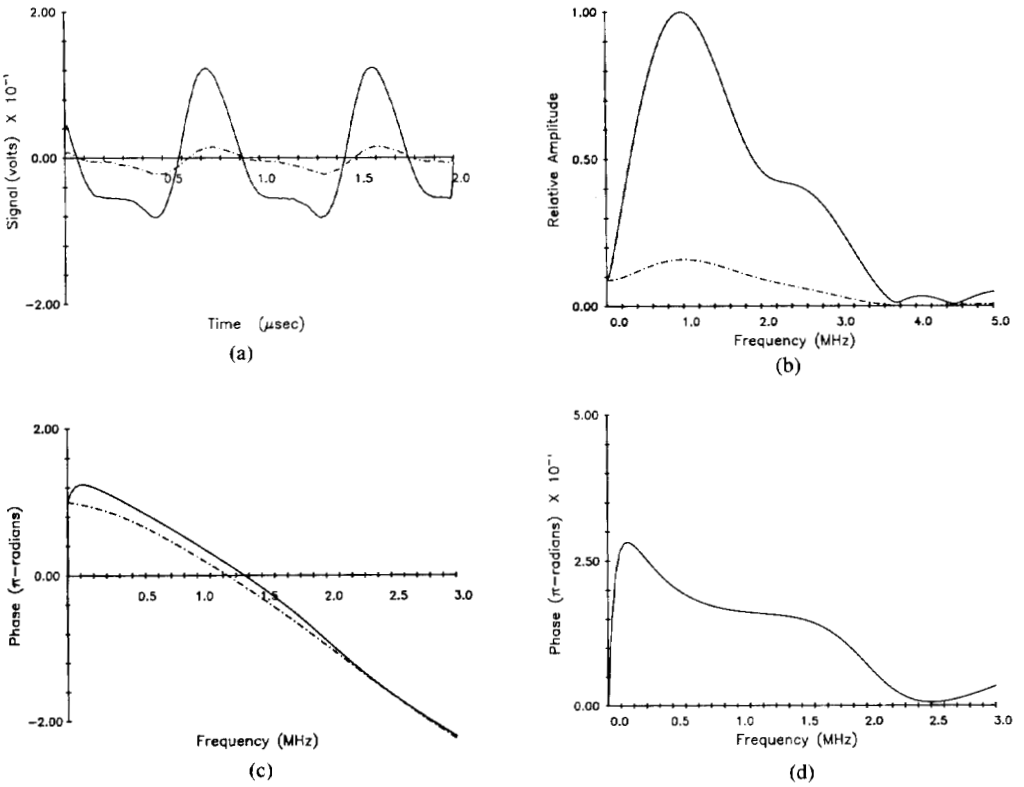

Fig. 8. Aperture effect of X-ray/acoustic signals in aluminum. (a) Waveforms corresponding to 4- and 24-mm (solid line) apertures. (b) Fourier magnitude spectra. (c) Fourier phase functions (unwrapped). (d) Phase difference between 4- and 24-mm-aperture phase functions.

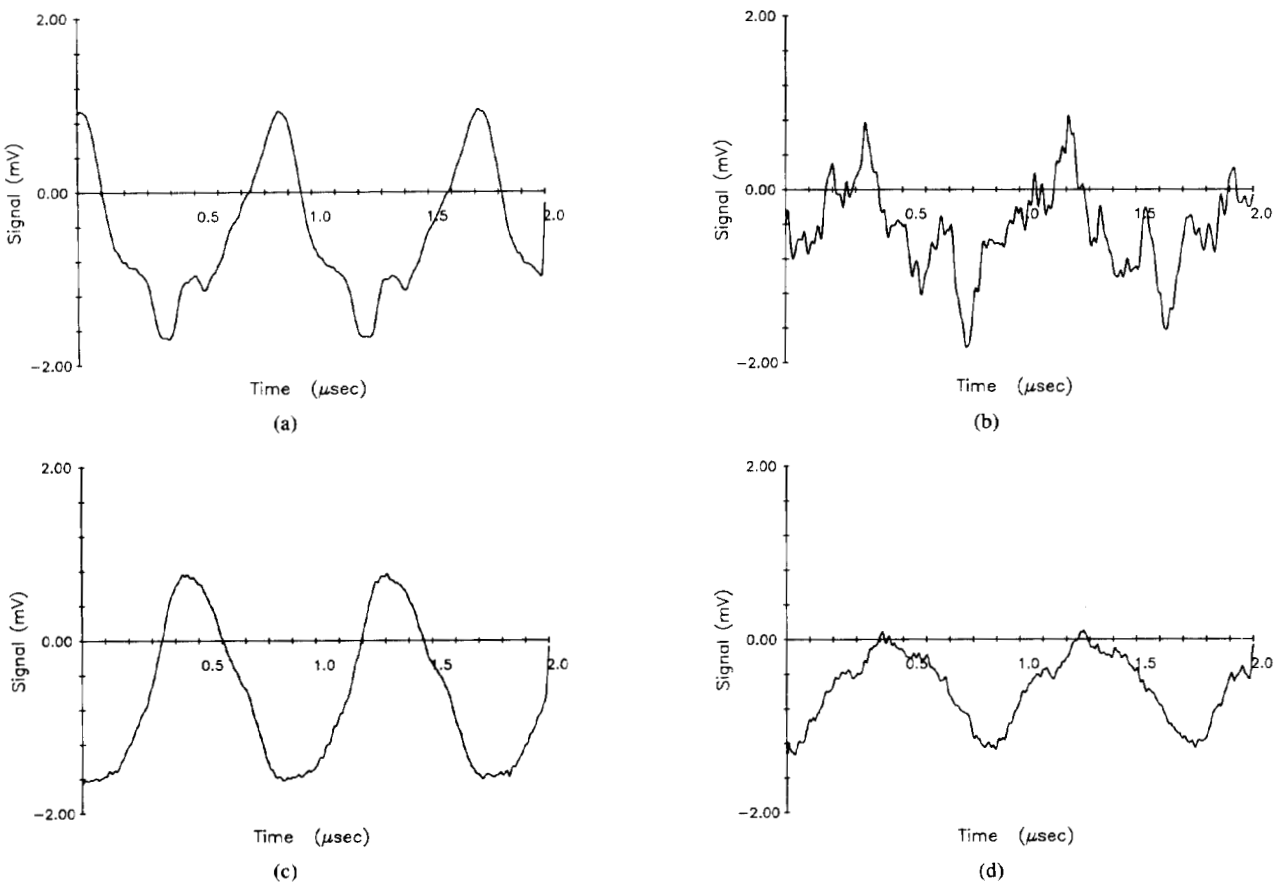

Fig. 9. X-ray/generated ultrasonic signals. (a) 0° (aligned with beam). (b) 30°. (c) 60°. (d) 90° (perpendicular to beam).

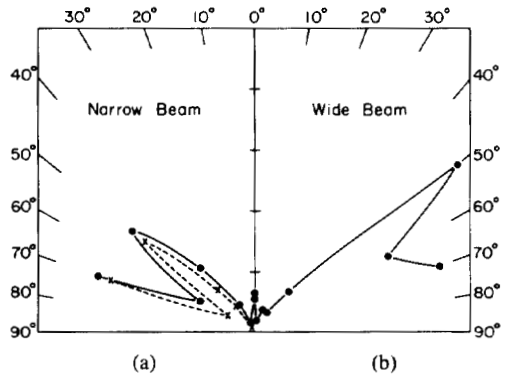

Fig. 10. Measured X-ray/acoustic signal directivity. (a) Wide-aperture X-ray beam. (b) Two tests with narrow aperture beam.

tation source repetition rate. Furthermore, it was observed that for particular orientations, specifically at 10°, 20°, and 30°, there appeared a complicated interference phenomenon in the detected signal which was not observed in the calibration experiment. To determine the directivity pattern, the amplitude of a particular ray arrival should be measured. However, the high synchrotron pulse repetition rate precludes this since the individual ray arrivals are not clearly identifiable. For this reason, only rms-signal amplitudes and peak-to-peak voltages were extracted from the waveforms.

Because some of the waveforms were small in amplitude and noise corrupted, it was found that the amplitude could be more reliably determined from the spectral magnitude corresponding to the frequency of the source excitation repetition rate, or 1.2 MHz. These amplitudes were normalized by the amplitude of the P-wave arrival signal determined from the calibration test. The results of the directivity so determined for two tests in which the X-ray beam was approximately 2 × 2 mm in cross section are shown in Fig. 10. It is observed that this radiation pattern resembles that of a dipolar point source. These results are similar to those which have been reported by Hutchins *et al.* [17] for a focused laser operating as a thermoelastic source on a specimen. The large amplitude values found above 80° are not reliable and hence they are excluded from the data shown. The amplitudes above these angles appear to be a direct result of the small *P*-wave amplitude measured at these orientations during the calibration test. It is likely that the piezoelectric point transducer used in the calibration test was not operating as a perfect monopolar source type. For comparison, also shown in Fig. 10 is the case of a broad X-ray beam whose cross-section was approximately 2 × 15 mm. The essential features here are similar to the narrow beam case, but the peak in directivity observed at approximately 50° is much higher in amplitude.

F. Double-Modulated X-Ray/Acoustic Signals

The use of modulated continuous wave thermal sources to generate thermal as well as thermoelastic waves in solids is becoming well established [18]. It was previously predicted that X-rays could be used similarly for thermoacoustic imaging applications [19]. But to the best of our knowledge, this has not yet been reported. As described in Section III-A, the high X-ray pulse repetition rate at the CHESS facility precludes recovery of details of the X-ray/acoustic source from the generated ultrasonic signals with existing signal processing algorithms. An alternative method, analogous to the existing thermoacoustic imaging methods but based on a double-modulation scheme, is proposed here.

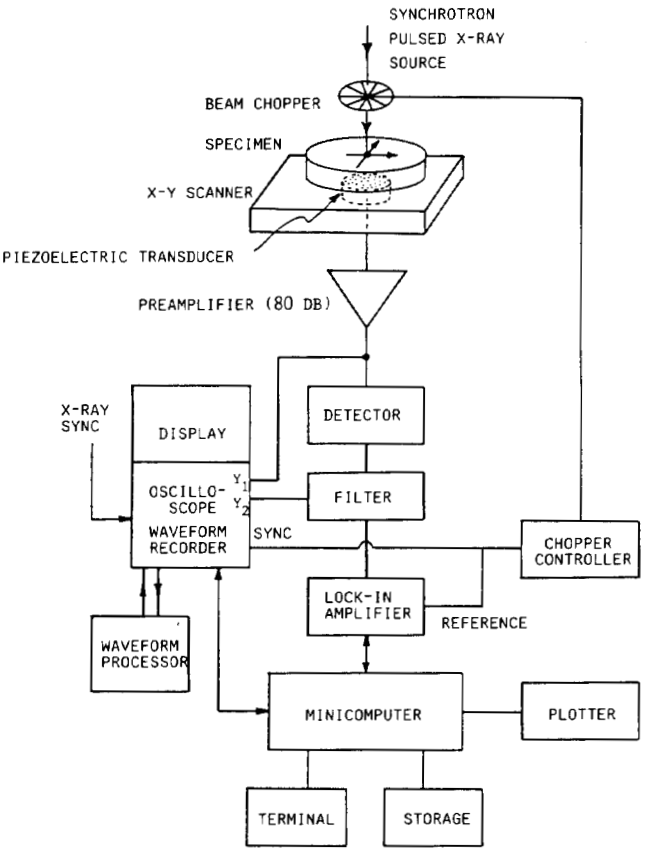

Fig. 11. X-ray/acoustic measurement system for real-time waveform acquisition and double-modulation tests.

To increase the thermal wavelength and hence the penetration depth of the thermal waves, it is possible to superimpose a low-frequency (kilohertz modulation) on the megahertz X-ray pulse repetition rate. The experimental system used for doing this is shown in Fig. 11. As shown, the system is capable of operating in several modes. In one, the system can record and process real-time X-ray-generated ultrasonic signals detected with a piezoelectric transducer attached to a sample, similar to the elementary system shown in Fig. 1. In that mode, the output of the transducer is amplified and connected directly to a processing oscilloscope or waveform recorder. A typical waveform detected in aluminum is shown in Fig. 12(a), which was synchronized to the X-ray pulse excitation rate. The addition of the beam chopper with a stainless steel blade superimposes a second modulation on the X-ray pulses, which is a thousand times lower in frequency. Attempts were made initially to synchronize the second modulation with the X-ray beam, but the stability require-

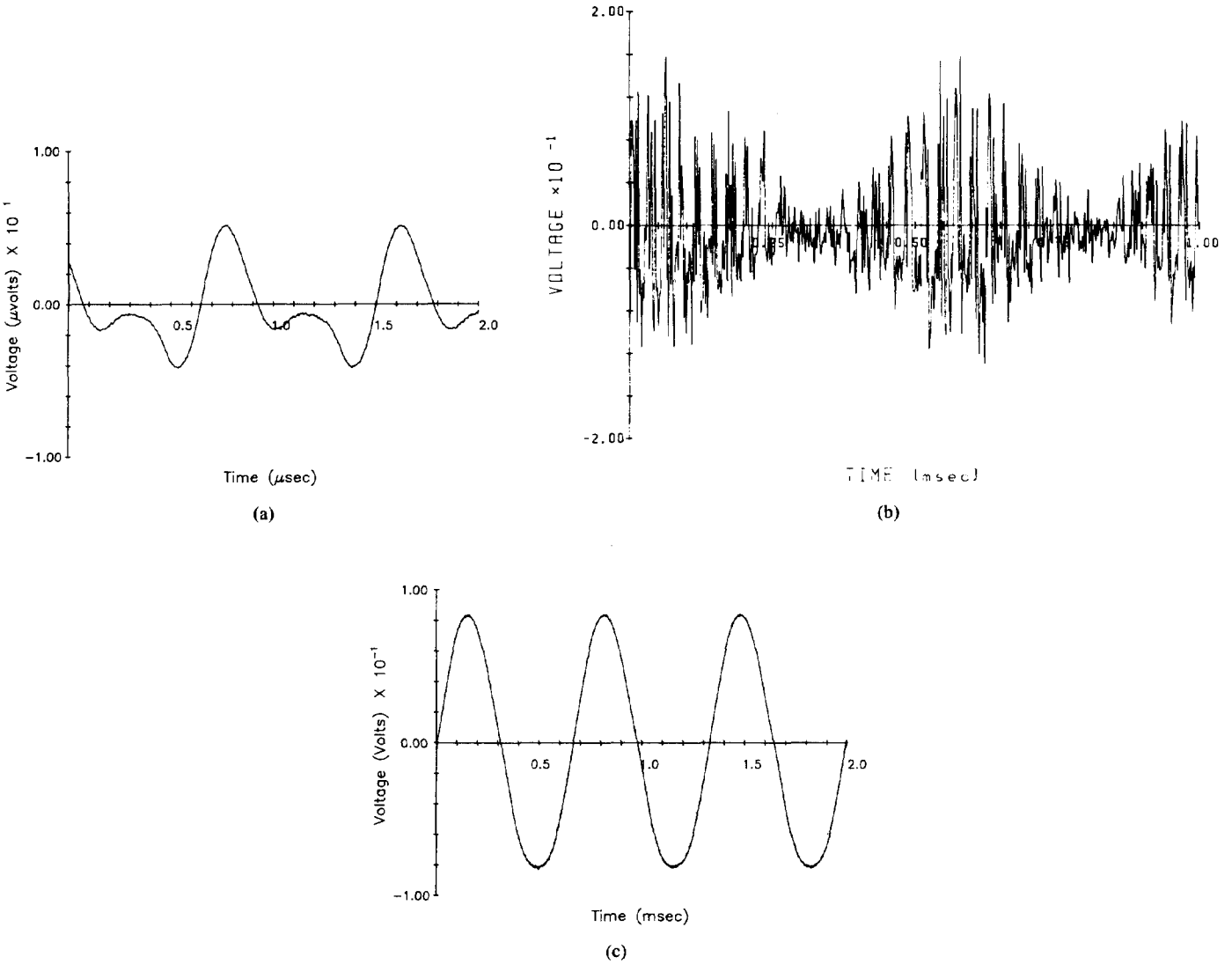

Fig. 12. Direct and modulated X-ray/acoustic signals in aluminum with slanted hole. (a) Direct signal. (b) Modulated direct signal (2 cycles; modulation frequency: 1.5 kHz). (c) Modulation envelope.

ments placed on the mechanical chopper are difficult to meet with existing chopper technology. As depicted in Fig. 12(b), approximately a thousand X-ray-generated ultrasonic pulses, unsynchronized with the modulation, are in each triangular-shaped modulation cycle. The time scale of this figure is a thousand times larger than that in Fig. 12(a). Using an envelope detector and filter, a quasi-periodic signal is obtained as shown in Fig. 12(c), whose frequency is the chopper modulation frequency and whose amplitude is directly related to the amplitude of the X-ray-generated acoustic signals. There is also a phase shift of these signals relative to the reference signal obtained from the chopper.

As in conventional thermal-wave imaging measurements, both the magnitude and phase of the detected signal can be easily recovered with a lock-in amplifier. It is also possible to use the waveform processing oscilloscope to quickly extract various waveform amplitude and time parameters from the detected signals. Data recording and subsequent data processing is facilitated by an attached minicomputer-based data acquisition system. By sweeping the modulation frequency, it is possible to generate an X-ray/acoustic signal spectrum, analogous to that determined in photoacoustic measurements in which the modulation frequency of a continuous thermal source is varied.

It is not yet clear whether the existing theories of thermal waves in solids (e.g., [20]) are applicable to interpret the signals measured with the technique described here. A principal difference is that the beam of X-rays is not continuous, but is rather a sequence of pulses 160 ps in duration with a repetition period of 850 ns. It is possible that interference phenomena between the thermal and thermoelastically generated ultrasonic waves may arise in thin specimens for particular source/receiver separations and specimen geometries. Also, since the frequency dependence of the thermal wavelength is proportional to $f^{-1/2}$ [13] while that of the elastic waves is proportional

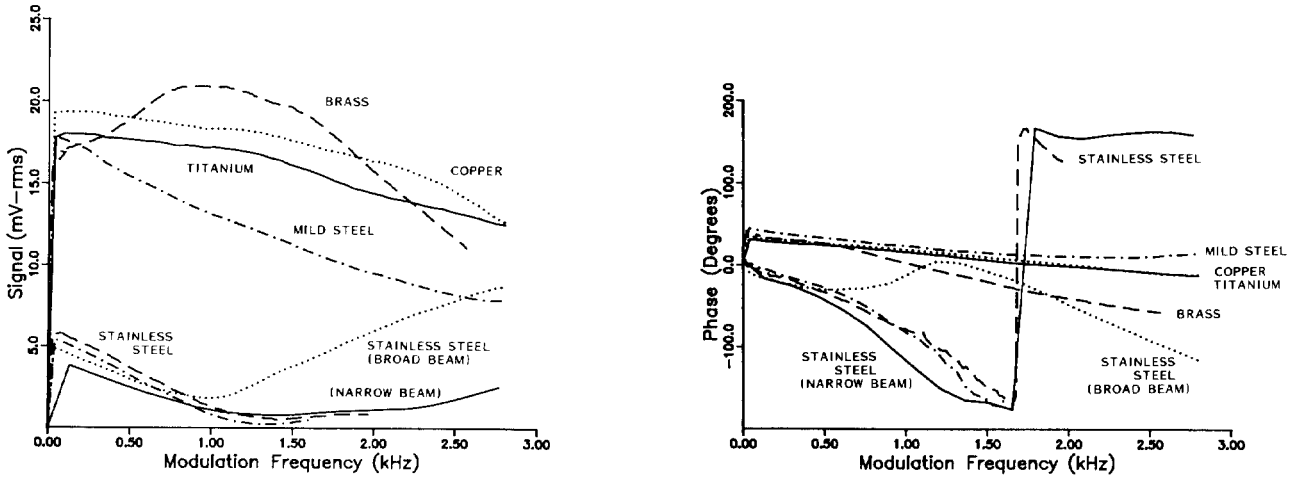

(a) (b)

Fig. 13. Results of double modulation experiments. (a) Magnitudes as a function of modulation frequency. (b) Phase as a function of modulation frequency.

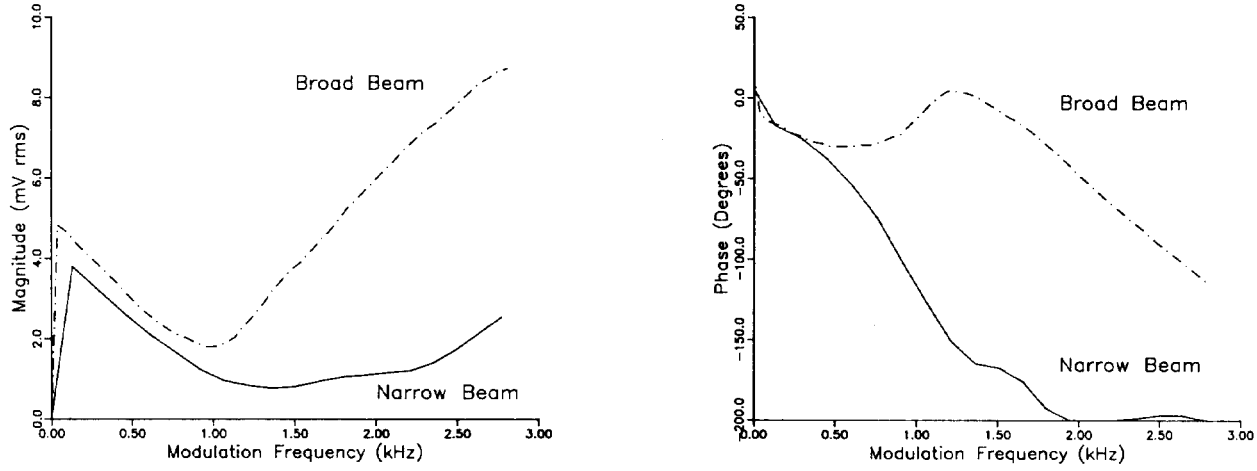

(a) (b)

Fig. 14. Beam size dependence of double modulated X-ray/acoustic signals in stainless steel. (a) Magnitude response. (b) Phase response.

to f^{-1}, these interferences may exhibit a complicated frequency dependence.

A first application of the modulated pulsed X-ray/acoustic technique was the determination of the magnitude and phase spectra of several metals. The results obtained for a scan of modulation frequency from zero to about 2.75 kHz is shown in Figs. 13(a)–(b). We note the reproducibility of the data from five repeat tests performed on a stainless steel specimen. The cross-section of the X-ray beam was approximately 2 × 2 mm, but the result of one test performed on the same specimen with an X-ray beam of broader cross-section gave the results indicated with a dotted line in Fig. 14(a). The decrease in magnitude A with increasing modulation frequency f shows that a power law of the form $A \propto f^{\alpha}$ can be fit to the data of most materials (Al, Cu, Ti, and mild and stainless steel), where α ranged from -0.3 to -0.6. The exceptions include brass with $\alpha = -1.5$ and several stainless steel specimens, which ranged from -1.3 to -2.5. The phase data shown in Fig. 14(b) indicate that those materials which exhibit the largest signal magnitudes also undergo the smallest phase change as the beam modula-

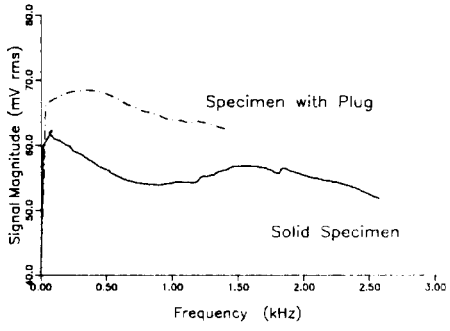

Fig. 15. Double modulation measurement of a solid aluminum specimen and one with a steel plug.

tion frequency is varied. The converse also appears to be true.

One experiment was completed with the aluminum disk specimen containing the steel plug in its interior, 12.5 mm from the front and rear surfaces. Fig. 15 shows a comparison of the magnitude spectra between a solid aluminum specimen and the imbedded pin specimen. Unfortunately, because of a beam dump, the data collection of the latter had to be terminated prior to reaching the maximum modulation frequency. Additional experiments with similar specimens are still needed to establish the potential and limitations of this new measurement technique.

IV. *X–Y* Scanning and Imaging

Using the measurement system depicted in Fig. 11, a series of scanning experiments was made in which specimens were moved in an x–y raster pattern in the X-ray beam, in which the cross section was approximately 2 × 2 mm in cross section. At each measurement, particular waveform parameters, such as voltage peak-to-peak, rms, mean, maximum, minimum, or others were extracted from the waveforms. As shown in Fig. 11, the measurement system permitted recording either data from real-time waveforms or the modulated X-ray/acoustic signals while scanning. The data acquisition software also permitted the scanning in various patterns, extracting, and acquiring up to three waveform parameters from the digital processing oscilloscope and/or recording entire waveforms at preselected or at all points along a scan line. Scanning resolution is currently restricted by the time between synchrotron fills and data acquisition rate, which is controlled by signal-averaging time.

In most of these experiments the ultrasonic signals were detected with a damped PZT transducer, either an 18.8 mm or a 1.3 mm diameter, mounted at the epicentral receiver position. Several additional experiments were made with the point sensor mounted on the side of the specimen. The scanned region typically covered the central 12 × 12 mm or 18 × 18 mm section of the disk, although some detailed scans were made along particular regions of interest.

Figs. 16(a)–(b) are the results obtained when the central region of a solid aluminum disk is scanned and the signals detected with the 1.3-mm PZT transducer mounted on the rear surface. Shown in Fig. 16(a) is the rms amplitude of the detected X-ray/acoustic signal. Since the specimen is homogeneous, we conclude from the measured sound field that the spatial variation of signal amplitude is either the result of wave propagation or resonance effects in the disk-like specimen or, in view of the pronounced circular symmetry, evidence of the detecting transducer's radiation pattern. A contour plot of the same data set, which is shown in Fig. 16(b), can be used to quickly extract dimensional features of the acoustic field.

Similar results were observed in the double-modulation experiments. An example using the identical measurement situation as above plus a superimposed second modulation at 1.5 kHz is shown in Fig. 17(a). As before, there is a spatial variation of signal amplitude that exhibits a circular symmetry. From a contour plot of this data it is seen that the spacing between the central peak and the annular ring is approximately the same as that observed in the earlier test. Thus, despite a significant change in thermal diffusion length, the detected signal is similar, pointing to the conclusion that the measured results must be principally due to the elastic wavefield of the specimen.

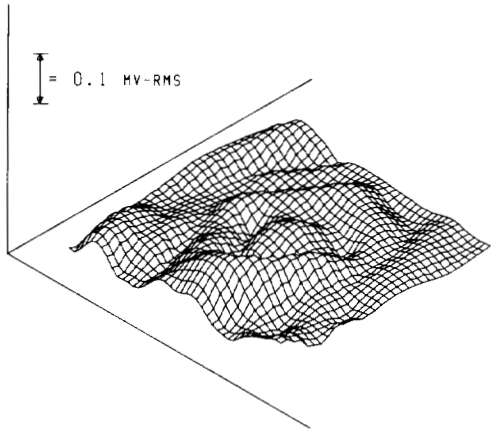

(a)

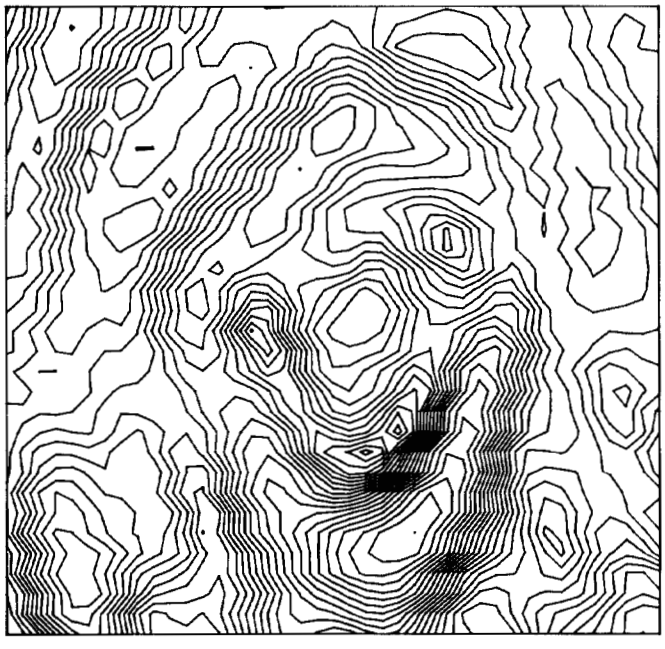

(b)

Fig. 16. x–y scan of a solid aluminum disk detected with a 1.3 mm piezoelectric transducer at epicenter. (a) rms signal amplitude. (b) Contour plot of (a).

At certain measurement points it was possible to observe the existence of a complicated wave interference phenomenon. The interference phenomenon appears in the detected waveforms as an apparent frequency, which is twice that detected at other positions. This is the case for

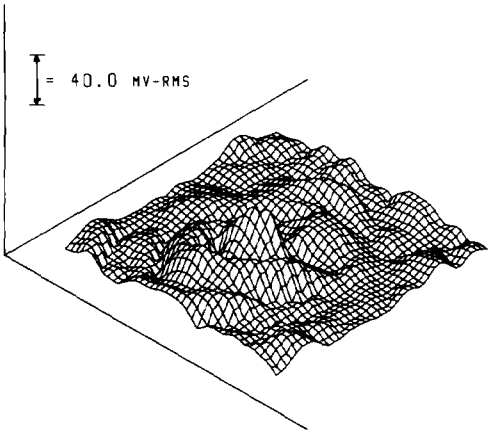

(a)

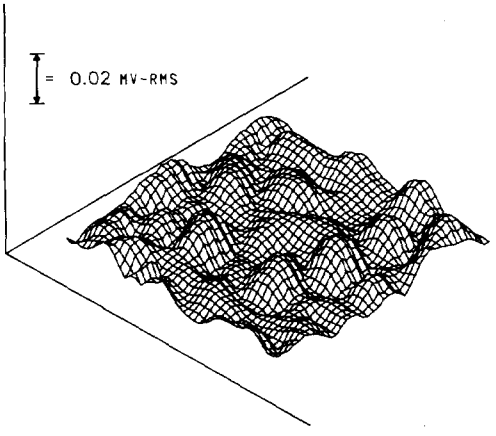

(b)

Fig. 17. Double modulation measurement of a solid aluminum disk. (a) Epicentral receiver. (b) Side-mounted receiver.

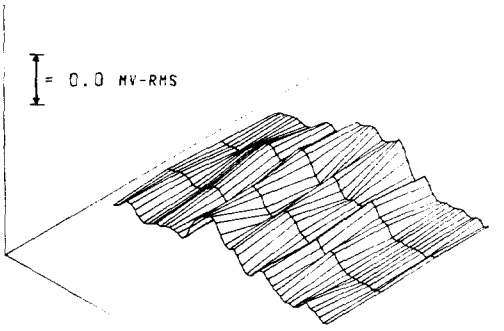

(a)

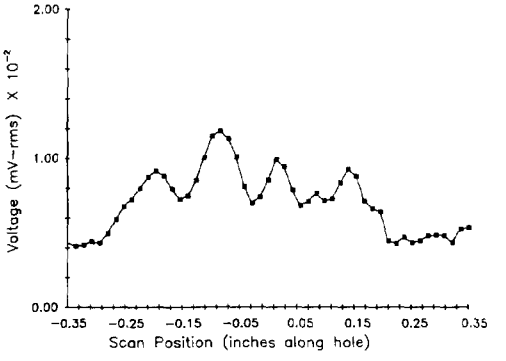

(b)

Fig. 18. *x–y* scan of an aluminum specimen containing a slanted hole. (a) rms level of X-ray/acoustic signal. (b) Signal amplitude along the axis of the slanted hole (line 3).

an out-of-phase interference occurring between two superimposed waveforms whose magnitude and phase are varying spatially. Similar observations were made in the scanned fields measured with a large diameter transducer. There is again an acoustic field with circular symmetry but with less pronounced maxima and minima than were observed with the smaller diameter piezoelectric transducer.

In Fig. 17(b) is the result obtained when the point piezoelectric transducer was mounted on the edge of the disk-like specimen 2.25 inches in diameter. The complicated interference pattern appears to be the result of an interference between various thermoelastically generated acoustic wave modes in the specimen. In very thin specimens, such inferences could, however, arise between the thermal and acoustic wave signals.

Scanned field measurements were also made on the disk-like specimens of aluminum possessing a variety of machined "flaws." As with the solid specimens, the waveform parameter extracted from the real-time acoustic signal or from the detected amplitude envelope of the double-modulation measurements exhibited a complicated spatial behavior, which overshadowed any details of the test feature of the specimen. The case of a scan of the slanted hole specimen is shown in Fig. 18(a). Here, the X-ray-generated acoustic signals were detected at the epicentral position of the specimen with a transducer 18.75 mm in diameter. The data values correspond to the rms signal amplitude of the detected waveforms. A periodicity in the scanned field is seen in Fig. 18(b) which exhibits features apparently dominated by the field characteristics of the transducer and the elastic resonances of the specimen.

It was observed in all the *x–y* scanning measurements that the sound fields appear to be dominated by elastic wave propagation effects. At megahertz frequencies the thermal wavelength is orders of magnitude smaller than the acoustic wavelength. But in the double-modulation measurements when the modulation frequency is low enough, the thermal-diffusion length is expected to be long enough to result in an interaction with the fabricated specimen features and to interfere as well with the thermoelastically generated signals. Since the piezoelectric detection scheme employed in these experiments detects signals consisting of both thermal and thermoelastic origins, further work analogous to that described by Murphy *et al.* [21] should be undertaken to delineate between the thermoelastic and the thermal contributions to the signals.

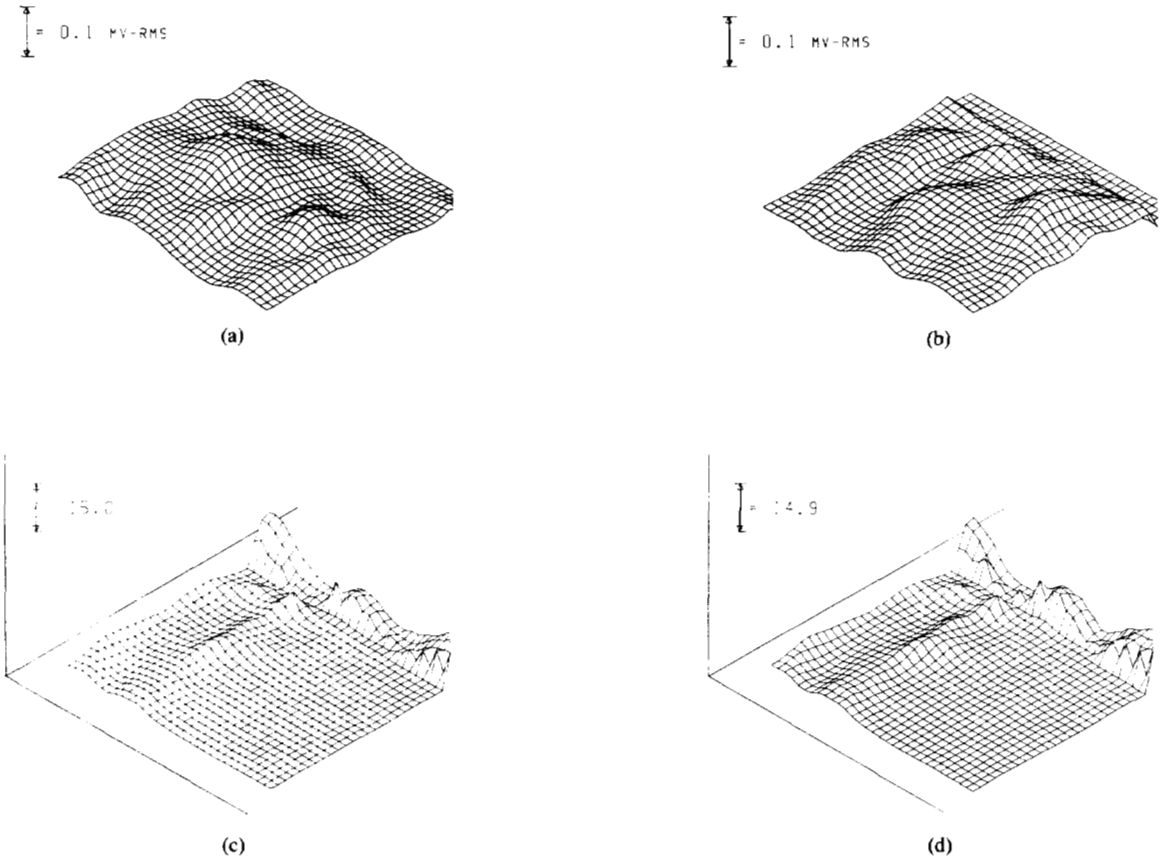

Fig. 19. x–y scan, double modulation measurement in an aluminum disk containing a slanted hole. (a) rms amplitude measured at 2.5 kHz modulation frequency. (b) rms amplitude measured at 0.5 kHz modulation frequency. (c) Amplitude ratio: 2.5 kHz/0.5 kHz. (d) Amplitude ratio: 1.5 kHz/0.5 kHz.

An alternate approach proposed here is a differential method in which X-ray acoustic signals are detected at two modulation frequencies of the pulsed X-ray beam. Thus measurements are made at two thermal diffusion lengths. If the wavelength of the thermoelastically generated ultrasonic signals is determined by the repetition rate of the synchrotron, then a ratio of the scanned fields made at two modulation frequencies permits a removal of the effects which are presumed to arise from the transducer and the specimen. The results obtained on the slanted hole specimen are shown in Fig. 19. In Figs. 19(a)–(b) are the scanned fields measured at 2.5 kHz and at 500 Hz, respectively. In the last three lines of the scan made at 500 Hz there was no X-ray beam. As before, it is difficult to perceive in each of these scanned fields features directly related to the slanted interior hole. However, by forming the ratio of these two scanned fields, Fig. 19(c) is obtained. Ignoring the region in which there was no beam, the region of the slanted hole is now apparent. As shown in Fig. 19(d), similar results are obtained when the ratio is formed from the data obtained at 500 Hz and 1.5 kHz. As this is only a preliminary result, additional measurements are needed to establish this method as a reliable means for using thermally generated, piezoelectrically detected signals to image interior inhomogeneities and microstructural features in materials.

V. Conclusion

The measurements reported here have confirmed the existence of X-ray-generated longitudinal and shear waves in specimens of a variety of metals. The signals were detected with piezoelectric transducers attached to disk-like specimens at epicentral as well as off-epicentral locations, out of the X-ray beam. In every case, the signals exhibited the time characteristics of the X-ray pulse repetition rate. At sufficiently low rates of excitation pulse repetition, a clear identification of specific elastic wave modes is possible in the detected signals.

Using the beam current of the synchrotron as a measure of the X-ray photon power, the beam current dependence of the X-ray-generated acoustic signals was established. When the X-ray beam is operating properly, the acoustic signals appear to be linearly related to the beam current and X-ray photon power. Hence, the measurements show that the X-ray/acoustic phenomenon can form the basis of an X-ray beam monitor sensor, sensitive to the X-ray photon power incident on a material.

Based on experiments in which the X-ray beamwidth

was adjusted by a variable slit, the amplitudes of the X-ray acoustic signals were found to depend linearly on the beam size to the extent up to the width of the receiving transducer. A Fourier phase analysis technique was demonstrated by which the extent of the X-ray/acoustic source could be estimated. The generated X-ray/acoustic signals measured in a large specimen show a directivity pattern independent of beam size resembling that of the thermoelastic signals generated by a pulsed thermal laser source.

A new double-modulation measurement technique was developed in which a mechanical chopper is used to modulate the pulsed X-ray beam. Waveform parameters such as rms, amplitude, and phase, were measured as a function of beam modulation frequency. It was found that the X-ray/acoustic spectra determined as a function of modulation frequency are material-dependent, analogous to the results previously obtained in laser-generated acoustic experiments.

Preliminary experiments were completed to explore the use of X-ray/acoustic signals to image material inhomogeneities. x–y scanning measurements were made in which features of the direct or double-modulated X-ray/acoustic signals are recorded as a function of position on a specimen. Similar results are obtained in both techniques. It was found that the measured scanned fields vary spatially, with features apparently dominated by the effects of the transducer and elastic wave resonances in the specimen. A preliminary test was completed with a new differential X-ray/acoustic measurement technique by which the effects of the elastic wave resonances are minimized so that spatial inhomogeneities such as a cylindrical hole in a specimen can be identified.

Acknowledgment

The use of the facilities at Cornell's High Energy Synchrotron Source (CHESS) is appreciated. Special thanks are due D. Mills at CHESS and V. Smith for help in preparing the manuscript. We acknowledge also the valuable discussions we have had with Drs. G. Busse and J. C. Murphy.

References

[1] W. Sachse and N. N. Hsu, "Ultrasonic transducers for materials testing and their characterization," in *Physical Acoustics* (vol. 14), W. P. Mason and R. N. Thurston, Eds. New York: Academic, 1979, pp. 277–405.

[2] C. B. Scruby, R. J. Dewhurst, D. A. Hutchins, and S. B. Palmer, "Laser generation of ultrasound in metals," in *Research Techniques in Nondestructive Testing* (vol. 5), R. S. Sharpe, Ed. New York: Academic, 1982, pp. 281–327.

[3] G. Birnbaum and G. S. White, "Laser techniques in NDE," in *Research Techniques in Nondestructive Testing* (vol. 7), R. S. Sharpe, Ed. New York: Academic, 1984, pp. 259–365.

[4] D. A. Hutchins and A. C. Tam, "Pulsed photoacoustic materials characterization," *IEEE Trans. Ultrason. Ferroelectrics Freq. Contr.*, vol. UFFC-33, pp. 429–449, 1986.

[5] H. N. G. Wadley, C. K. Stockton, J. A. Simmons, M. Rosen, S. D. Ridder, and R. Mehrabian, "Quantitative acoustic emission studies for materials processing," *Review of Progress in Quantitative Nondestructive Evaluation* (vol. 1), D. O. Thompson and D. E. Chimenti, Eds. New York: Plenum, 1982, pp. 421–431.

[6] G. Busse, "Imaging with optically generated thermal waves," *IEEE Trans. Sonics Ultrason.*, vol. SU-32, no. 2, pp. 355–364, 1985.

[7] A. Rosencwaig, "Applications of thermal wave physics to microelectronics," in *VLSI Electronics Microstructure Science* (vol. 9), N. Einspruch, Ed. New York: Academic, 1985, pp. 227–287.

[8] D. Kishoni and W. Sachse, "Spark-generated ultrasound," MSC Report no. 4752, Materials Science Center, Cornell University, Ithaca, NY, June 1982.

[9] G. S. Cargill, III, "Electron-acoustic microscopy," *Physics Today*, vol. 34, no. 10, pp. 27–32, 1981.

[10] F. G. Satkiewicz, J. C. Murphy, L. C. Aamodt, and J. W. Maclachlan, "Ion-acoustic imaging of subsurface flaws in aluminum," in *Proc. Rev. Progress in Quantitative NDE.* New York: Plenum, 1986.

[11] K. Y. Kim and W. Sachse, "X-ray generated ultrasound," *J. Appl. Phys. Lett.*, vol. 43, pp. 1099–1101, 1983.

[12] ——, "Observation of X-ray generated ultrasound," in *Proc. 1983 IEEE Ultrason. Symp.*, pp. 677–680, 1983.

[13] R. M. White, "Generation of elastic waves by transient surface heating," *J. Appl. Phys.*, vol. 34, pp. 3559–3567, 1963.

[14] C. Chang and W. Sachse, "Analysis of elastic wave signals from an extended source in a plate," *J. Acoust. Soc. Amer.*, vol. 77, no. 4, pp. 1335–1341, 1985.

[15] H. Y. Ko and R. F. Scott, "Deconvolution techniques for linear systems," *Bull. Seismol. Soc. Amer.*, vol. 57, pp. 1393–1408, 1967.

[16] W. Sachse and Y.-H. Pao, "On the determination of phase and group velocities of dispersive waves in solids," *J. Appl. Phys.*, vol. 48, no. 8, pp. 4320–4327, 1978.

[17] D. A. Hutchins, R. J. Dewhurst, and S. B. Palmer, "Laser generated ultrasound at modified metal surfaces," *Ultrasonics*, vol. 19, pp. 103–108, 1981.

[18] "4th International Topical Meeting on Photoacoustic, Thermal and Related Sciences," Ecole Polytechnique de Montreal, Aug. 1985.

[19] A. Rosencwaig, *Photoacoustics and Photoacoustic Spectroscopy.* New York: John Wiley, 1980, p. 297.

[20] J. Opsal and A. Rosencwaig, "Thermal wave depth profiling: Theory," *J. Appl. Phys.*, vol. 53, p. 4240, 1982.

[21] J. C. Murphy, J. W. Maclachlan, and L. C. Aamodt, "Image contrast processes in thermal and thermoacoustic imaging," *IEEE Trans. Ultrason. Ferroelectrics Freq. Contr.*, vol. UFFC-33, pp. 529–541, 1986.

Wolfgang Sachse (M'76) was born on March 22, 1942 in Berlin-Charlottenburg, Germany. He received the B.S. degree in physics from Pennsylvania State University and the M.S.E. and Ph.D. degrees in 1966 and 1970, respectively, in mechanics and materials science from The John Hopkins University, Baltimore, MD.

He is a Professor in the Department of Theoretical and Applied Mechanics at Cornell University and a member of the Materials Science Center. He was a German Government Academic Exchange Fellow in 1969/70 at the Institut für Metallkunde und Metallphysik at the Technische Hochschule, Aachen, Federal Republic of Germany. In 1977/78 he spent a sabbatical year at the Institute for Materials Research at the National Bureau of Standards. His current research interests include experimental work in ultrasonics, physical acoustics, and the nondestructive testing of materials. For the past 15 years, he has been engaged in studies of ultrasonic characterization of composite materials, the scattering of ultrasonic waves by various obstacles in elastic media, acoustic emission, the visualization of elastic waves by optical techniques, acoustoelasticity and the ultrasonic measurement of residual stresses, and spark- and X-ray-generated ultrasound for imaging of material inhomogeneities and microstructures.

Dr. Sachse is a member of the Acoustical Society of America, the American Society of Non-destructive Testing (ASNT), Sigma Xi, the Society for Experimental Mechanics (SEM), and the Acoustic Emission Working Group (AEWG). He serves currently as chairman of the Acoustic Emission Working Group.

Kwang Yul Kim was born in South Korea on September 2, 1942. He received the B.Sc. degree in nuclear engineering from Seoul National University in 1966 and the Ph.D. degree in materials science and engineering from Cornell University, Ithaca, NY, in 1975.

He is currently a Senior Research Associate at Cornell University in the Department of Theoretical and Applied Mechanics. His interests are in the areas of characterization of various acoustic emission sources, wave propagation, and nondestructive testing.

Wilbur F. Pierce IV was born in Buffalo, NY, on July 4, 1965.

After attending his freshman year at the Rochester Institute of Technology, he transferred to Cornell University and is currently enrolled as a Junior in the School of Applied and Engineering Physics. His interests lie in solid state physics and applied mathematics.

Mr. Pierce is a member of Tau Beta Pi.